RSC Advances

PAPER

View Article Online
View Journal | View Issue

Check for updates

Cite this: *RSC Adv.*, 2023, **13**, 2833

Induction of toxicity in human colon cells and organoids by size- and composition-dependent road dust†

Sung Bum Park,‡[a] Eun-Ah Kim,‡[b] Ki Young Kim*[a] and Byumseok Koh *[a]

Received 25th November 2022
Accepted 3rd January 2023

DOI: 10.1039/d2ra07500h

rsc.li/rsc-advances

Environmental pollution, including the annual resurgence of particulate matter derived from road dust, is a serious issue worldwide. Typically, the size of road dust is less than 10 μm; thus, road dust can penetrate into human organs, including the brain, through inhalation and intake by mouth. Therefore, the toxicity of road dust has been intensively studied *in vitro* and *in vivo*. However, *in vitro* systems, including 2D cell cultures, cannot mimic complex human organs, and there are several discrepancies between *in vivo* and human systems. Here, we used human colon cells and organoids to evaluate the cytotoxicity of particulate matter derived from road dust. The toxicity of road dust collected in industrialized and high traffic areas and NIST urban particulate matter reference samples were evaluated in 2D and 3D human colon cells as well as colon organoids and their characteristics were carefully examined. Data suggest that the size and elemental compositions of road dust can correlate with colon organoid toxicity, and thus, a more careful assessment of the size and elemental compositions of road dust should be conducted to predict its effect on human health.

Open Access Article. Published on 18 yanvar 2023. Downloaded on 01.01.2025 04:59:55.
This article is licensed under a Creative Commons Attribution-NonCommercial 3.0 Unported Licence.

Introduction

Particulate matter toxicity derived from road dust has been a great concern, as the amount of road dust in the air has increased dramatically due to industrial and transport-induced production of air pollutants.[1,2] Previous studies have shown that road dust consists of various chemicals, including carbonaceous materials, metals, organic matter and ions.[3,4] Various studies have reported road dust-induced toxicity *in vitro* and *in vivo* as well as its impact on human health.[5,6]

As road dust is also present in the air, the human respiratory system, oral intake system and skin can be directly exposed to road dust.[7,8] In particular, due to its small size, particulate matter derived from road dust can enter digestive system through oral uptake.[9,10] Previous environmental monitoring studies have reported that particulate matter can induce toxicity in the human gastrointestinal (GI) tract and cause diseases, including inflammatory bowel diseases.[11–14] An *in vivo* study also suggested that particulate matter also triggers intestinal inflammatory responses in the murine intestine.[15] Therefore, carefully analyzing the influence of road dust on the human GI tract is necessary, and a tool for evaluating road dust-induced toxicity in the human digestive system is needed.

Organoids are three-dimensional self-organizing cell cultures derived from tissues or stem cells (embryonic or induced pluripotent).[16,17] Organoids exhibit differentiation and self-renewal abilities that allow them to closely mimic the microanatomy of the complexity of an actual organ.[18,19] Organoids can be derived from both normal or disease tissues or stem cells, allowing us to understand material-induced toxicity and its mechanisms.[20,21] *In vitro* systems for evaluating cytotoxicity from toxic substances have evolved from normal flat cell culture to 3D culture and organoids. 3D culture more closely mimics 3D tissue nature, and organoids are capable of recapitulating key features of organs, as they consist of multiple organ-specific cell types depending on the type of differentiation. When evaluating toxicity from substances, organoids exhibit several advantages, such as 2D and 3D *in vitro* systems, and even *in vivo* animal study results often do not correlate with human responses. In addition, *in vivo* studies have been greatly regulated recently due to increased concern about animal rights. Therefore, systematic comparison studies that evaluate road dust toxicity using 2D, 3D and human organoids are necessary to develop an appropriate system. Road dust is not homogeneous and has different sizes and compositions. Although several careful studies have been reported regarding road dust-induced cytotoxicity and its influence on human health,[22,23] relationships between road dust particle

[a]*Biotechnology and Therapeutics Division, Korea Research Institute of Chemical Technology, 141 Gajeong-ro, Yuseong-gu, Daejeon 34114, Republic of Korea. E-mail: kykim@krict.re.kr; bkoh@krict.re.kr*

[b]*National Assembly Futures Institute, Members Office Bldg, 1 Uisadang-daero, Yeongdeungpo-gu, Seoul, 07233, Republic of Korea*

† Electronic supplementary information (ESI) available. See DOI: https://doi.org/10.1039/d2ra07500h

‡ These authors equally contributed to this work.

© 2023 The Author(s). Published by the Royal Society of Chemistry

Open Access Article. Published on 18 yanvar 2023. Downloaded on 01.01.2025 04:59:55.
This article is licensed under a Creative Commons Attribution-NonCommercial 3.0 Unported Licence.

characteristics and toxicity are rarely reported and should be carefully monitored.

Here, we conducted a systematic evaluation of road dust-induced toxicity in 2D and 3D colon fibroblast and human colon organoids and monitored road dust size- and constituent-dependent toxicity. In addition, the road dust-induced inflammatory response in human colon organoids was carefully examined. The purpose of our study was to reveal the relationship between road dust characteristics and cytotoxicity and find potential for using human organoids for toxicity evaluation systems.

Results and discussion

Size and surface charge of road dust

The particle size, charge distribution of the road dust samples including National Institute of Standards and Technology (NIST) reference particulate matter (SRM 1648a) were examined. According to particle size distribution analysis data, the average diameters of the road dust samples we examined were in the range between 9.37 and 115.88 μm, with the smallest SRM1648a and the largest road dust 3 (Fig. 1A and B). Although we originally fractionated the road dust 1–4 samples and NIST reference sample to have a 50% cut-off point of 2.5 μm in aerodynamic diameter, the road dust samples may be aggregated and become larger in size due to noncovalent interactions, probably during the stirring period. The average zeta potential of road dust ranged between −12.72 and −20.94 mV (Fig. 1C). Although particle size and zeta potential are generally unrelated, Fig. 1B and C indicate that the average particle size and average zeta potential have a positive correlation. Because the zeta potentials of the road dust were within the agglomerating range,[24] the road dust particle size distribution might have been affected by surface charge. Due to this positive correlation, the particle size and zeta potential may have a confounding effect on toxicity. However, we need more road dust samples to generalize this observation.

Elemental compositions of road dust

Elemental compositions of road dust were analysed (Table S1†). Previous studies[25,26] have shown that road dust contains various chemical compounds, including organic carbons, sulfur compounds, metals and ions. These studies showed that metal compositions and the relative abundance of hydrocarbons have positive correlations with cytotoxicity and that the chemical profile of road dust may be used as a proxy for assessing human health impacts. Other studies also suggested that carbonaceous compounds, which account for approximately 3–26% of road dust, may have serious long-term impacts on human health.[27,28] Road dust also contains a significant amount of sulfur compounds, which can be beneficial when encountered in food but can cause reduced heart and lung diseases when present in road dust.[29] Chronic exposure to Pb in road dust can cause brain and central nervous system malfunctions.[30,31] Based on the findings regarding the toxic constituents of road dust, we determined that carbon (C), sulfur (S) and lead (Pb) are the key elements affecting human colon toxicity, and the C, S, and Pb compositions of each road dust are summarized in Table 1. In this study, we intended to investigate whether these elemental compositions could also be related to the toxicities in human colon cells and organoids. The C, S, and Pb compositions are positively correlated with each other and with the particle size or zeta potential. Therefore, it is impossible to single out the influence of each component in road dust on the overall

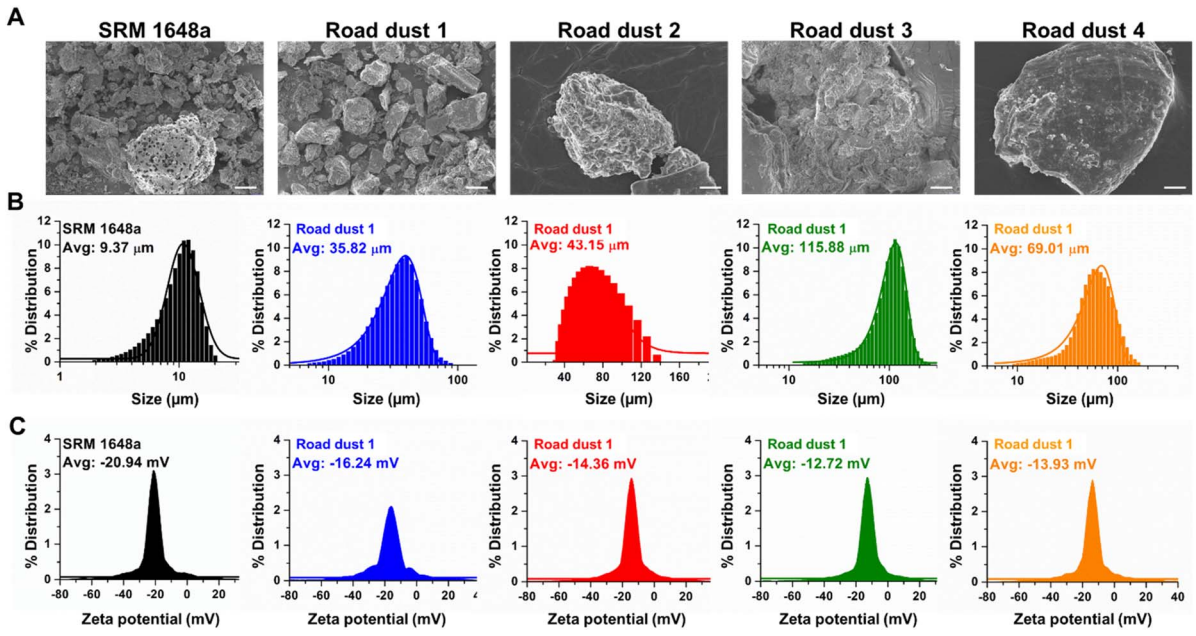

Fig. 1 Characterization of road dust (A) SEM images, (B) particle size distribution and (C) zeta potential distribution of SRM1648a, road dust 1, 2, 3 and 4. Scale bars represent 5 μm.

© 2023 The Author(s). Published by the Royal Society of Chemistry

Open Access Article. Published on 18 yanvar 2023. Downloaded on 01.01.2025 04:59:55.
This article is licensed under a Creative Commons Attribution-NonCommercial 3.0 Unported Licence.

Table 1 The C, S and Pb compositions (wt%) of road dust

	C (wt%)	S (wt%)	Pb (wt%)
SRM 1648a	12.70	5.51	0.66
Road dust 1	6.33	1.05	0.15
Road dust 2	5.99	0.84	—
Road dust 3	4.72	0.58	0.06
Road dust 4	4.92	0.96	0.08

toxicity. Instead, a generalized linear mixed model could be adopted to approximate a combined toxicity from various toxicants present in road dust.[32] Setting the computational details aside, the model equation assumes that the mixture toxicity is a linear combination of each toxic constituent's toxicity with additional terms accounting for joint impacts from various pairs of multitoxicants. We could qualitatively infer which physico-chemical property is strongly correlated with road dust toxicity based on the coefficients and R^2 obtained from the dose–response graph.

Road dust induced toxicity in 2D colon fibroblasts

To investigate road dust-induced toxicity in human colon cells, we exposed various road dust to CCD-18Co normal colon fibroblast cells. Road dust induced concentration-dependent toxicity, as the highest concentration we tested (2 mg mL^{-1}) showed a 20.2% (road dust 3) to 60.1% (SRM 1648a) decrease in CCD-18Co viability (Fig. 2A and B). Study by Feng *et al.* suggests quantification of the interactions among metal mixtures in toxicity with linear models.[33] Road dust toxicity and S, Pb, C contents showed generally positive correlations, which may indicate relationship between the chemical contents and fibroblastic cytotoxicity of road dust (Fig. 2C). Particle size showed a strong linear relationship ($y = 0.35x + 43.26$ with an R^2 value of 0.93) with cytotoxicity, as a smaller road dust induced higher toxicity to cells (Fig. 2D). In previous studies, it was suggested that smaller particles tend to accumulate and easily enter cells,[34,35] and smaller road dust can be more easily endocytosed or penetrate inside cells, causing cell damage and cell death. Colon cell cytotoxicity also showed a strong relationship with road dust surface charges, as road dust with stronger surface charges induced more cell death (R^2 value: 0.88, Fig. 2E). Many studies have shown that the surface charge of nanoparticles has a strong relationship with cell entry and penetration.[36,37] Although not conclusive, our data suggest that compared to the surface charge of the road dust, the size and constituent of the road dust are more critical.

Road dust induced cytotoxicity in 3D colon fibroblasts

Cells in human organs occur in the 3-dimensional type. We formed 3D spheroids with colon normal fibroblast CCD18-Co and exposed them to road dust. The cytotoxicity of road dust in 3D spheroids was less than that in 2D cultures, as 2 mg mL^{-1} road dust samples induced 43.1 (SRM 1648a) – 23.2 (road dust 3) % cell death (Fig. 3A and B). This is probably because road dust exposure to colon cells is limited in 3D spheroids compared to 2D cultures, as the total exposed surface area of cells was smaller than that of flat 2D cultures when the same number of cells were present. Similar to 2D culture, S-, Pb- and C-dependent toxicity was observed (Fig. 3C), as increasing the % composition of these three elements in road dust was positively related to 3D colon spheroid toxicity. The size and charge of the road dust were also major factors of spheroid cytotoxicity, as a smaller road dust with a more negative surface charge induced greater cytotoxicity (R^2 values: 0.78 and 0.90, respectively, Fig. 3D and E). Overall, we observed a similar tendency between 2D and 3D colon fibroblast cytotoxicity in the presence of road dust.

Influence of road dust in colon organoids

Next, we monitored the influence of road dust in colon organoids. Colon organoids derived from induced pluripotent stem

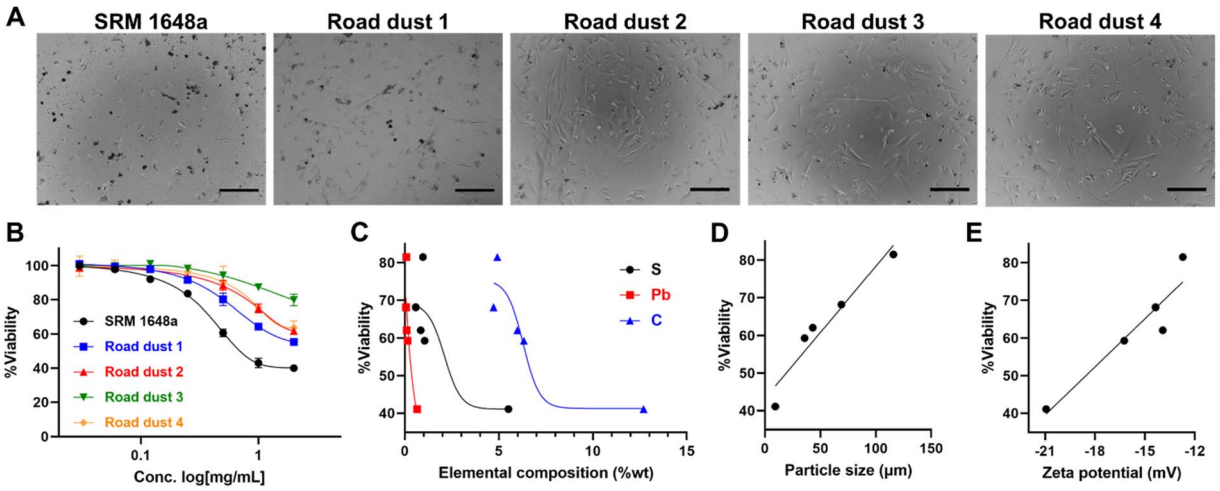

Fig. 2 Road dust-induced toxicity in 2D colon fibroblasts. (A) Bright field (BF) images of 2D colon fibroblasts upon addition of road dust. (B) Road dust concentration. (C) Elemental composition. (D) Particle size. (E) Zeta potential *vs.* 2D cell viability. Error bars represent the standard deviation from three independent experiments. Scale bars represent 20 μm.

Open Access Article. Published on 18 yanvar 2023. Downloaded on 01.01.2025 04:59:55.
This article is licensed under a Creative Commons Attribution-NonCommercial 3.0 Unported Licence.

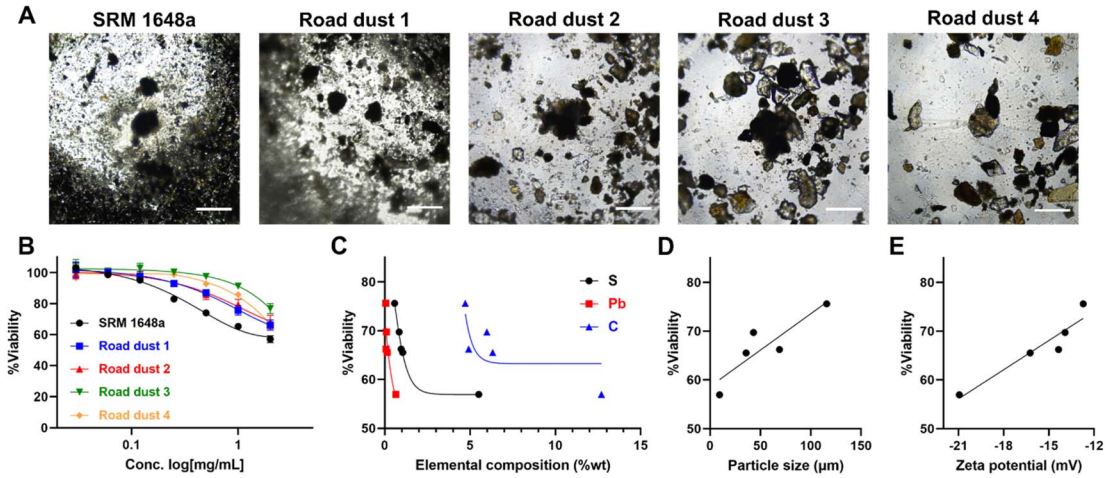

Fig. 3 Road dust-induced toxicity in 3D colon fibroblasts. (A) BF images of 3D colon fibroblast spheroids upon addition of road dust. (B) Road dust concentration. (C) Elemental composition. (D) Particle size. (E) Zeta potential *vs.* 3D colon fibroblast viability. Error bars represent the standard deviation from three independent experiments. Scale bars represent 20 μm.

cells (iPSCs) were cultured in the presence of Matrigel for 9 days. Differentiated colon organoids expressed specific colon markers resembling the actual human colon {leucine-rich repeat-containing G-protein coupled receptor 5 (LGR5), mucin-2 (MUC2), homeobox protein CDX-2 (CDX2), villin, Ki67, Fig. S1†}. SRM 1648a and road dust 1–4 (2 mg mL^{-1}) were

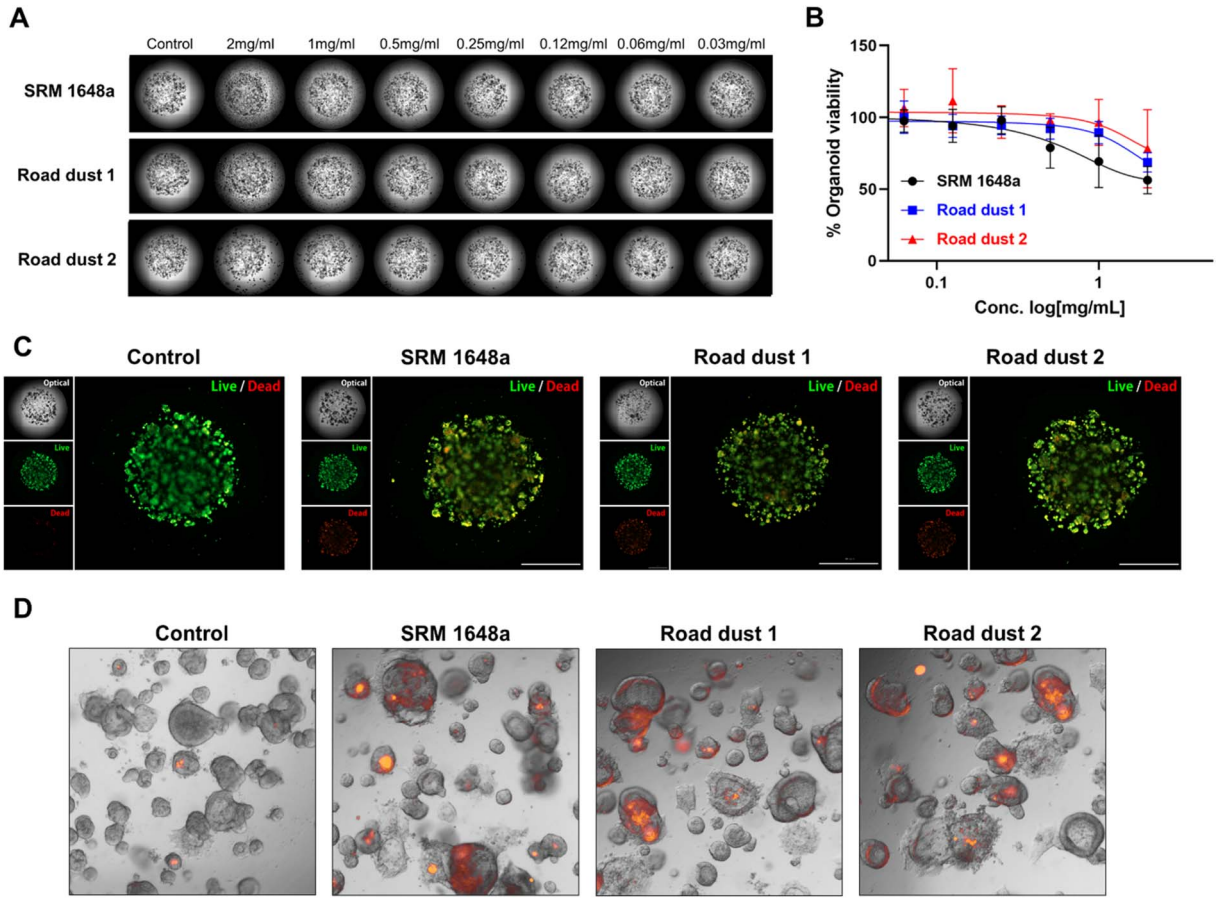

Fig. 4 Road dust-induced toxicity in human colon organoids. (A) BF images of human colon organoids upon addition of road dust. (B) Road dust concentration *vs.* colon organoid viability. (C) Colon organoid live/dead assay. (D) Fluorescence images of colon organoid oxidative stress responses. Error bars represent the standard deviation from three independent experiments.

© 2023 The Author(s). Published by the Royal Society of Chemistry

Open Access Article. Published on 18 yanvar 2023. Downloaded on 01.01.2025 04:59:55.
This article is licensed under a Creative Commons Attribution-NonCommercial 3.0 Unported Licence.

incubated with human colon organoids, and their effect on organoid viability was recorded (Fig. S2†). Among the 5 road dust we tested, three road dust inducing more cytotoxicity in 2D and 3D human colon fibroblasts (SRM 1648a, 1 and 2) were selected, and various concentrations of those road dust were exposed to colon organoids, and the impact on human colon organoids was monitored (Fig. 4A and B). Similar to human colon fibroblasts, road dust size- and constituent-dependent cytotoxicity were observed in colon organoids (Fig. S3†). Smaller road dust particles with higher % compositions of C, S and Pb were observed in colon organoids. Smaller road dust particles may easily penetrate colon organoids, and the C, S and Pb contained in road dust may induce colon organoid toxicity. Accumulation of some road dust outside of Matrigel was also observed, and larger road dust particles may not be able to penetrate Matrigel, thus these particles induce less cytotoxicity. In addition, although colon organoids consisted of many diverse cell types that resemble actual human organs, their cytotoxicity pattern with road dust showed similar results as those of CCD18-Co. This may suggest that road dust's size and constituent are key factors of road dust-induced cytotoxicity regardless of colon cell types. To confirm the effect of road dust size and composition on the cytotoxicity of colon organoids, a live/dead (LD) assay was conducted. The data suggest that the addition of SRM 1648a and road dust 1 and 2 induced the death of human colon organoids (2 mg mL^{-1}, Fig. 4C). It has been suggested that road dust induces oxidative stress in cells and tissues by modulating the oxidation–reduction (redox) cycle.[38,39] Oxidative stress through the production of reactive oxygen species (ROS), which is induced by the presence of road dust, leads to inflammatory responses and eventual cell death. Our data confirm that in the presence of 2 mg mL^{-1} SRM 1648a, road dust 1 and 2, ROS are generated in human colon organoids (Fig. 4D). Taken together, these results confirmed that road dust induces ROS generation in human colon organoids, resulting in oxidative stress, which may lead to an inflammatory response and inflammatory bowel diseases (IBDs) in the human colon.

Road dust induced an inflammatory response in human colon organoids

As previous data showed potential inflammatory responses in human colon organoids in the presence of road dust, IBD-focused polymerase chain reaction (PCR) array analysis of road dust-exposed human colon organoids was conducted. PCR array experimental data showed that colon organoids exposed to road dust induced changes (>2-fold changes according to the manufacturer's suggestion) in 13 inflammatory-related genes among 84 genes (Table S2†). Among those 13 genes, the expression levels of 12 genes were increased. We further conducted a quantitative PCR (qPCR) experiment to confirm the PCR array results. The data suggested that upon addition of 2 mg mL^{-1} SRM 1648a and road dust 1, the expression levels of 12 inflammatory-related genes from PCR array analysis were all increased in the qPCR results (Fig. 5). Among those inflammation-related genes in which the expression levels were increased upon addition of road dust, the complement component 3 (C3) gene is related to activation of the complement system, which is part of the immune system.[40] Chemokine (C–C motif) ligand 20 (CCL20) is a strong chemoattractant for lymphocytes and attracts neutrophils and is thus associated with inflammatory activation. Chemokine (C–X–C motif) ligand

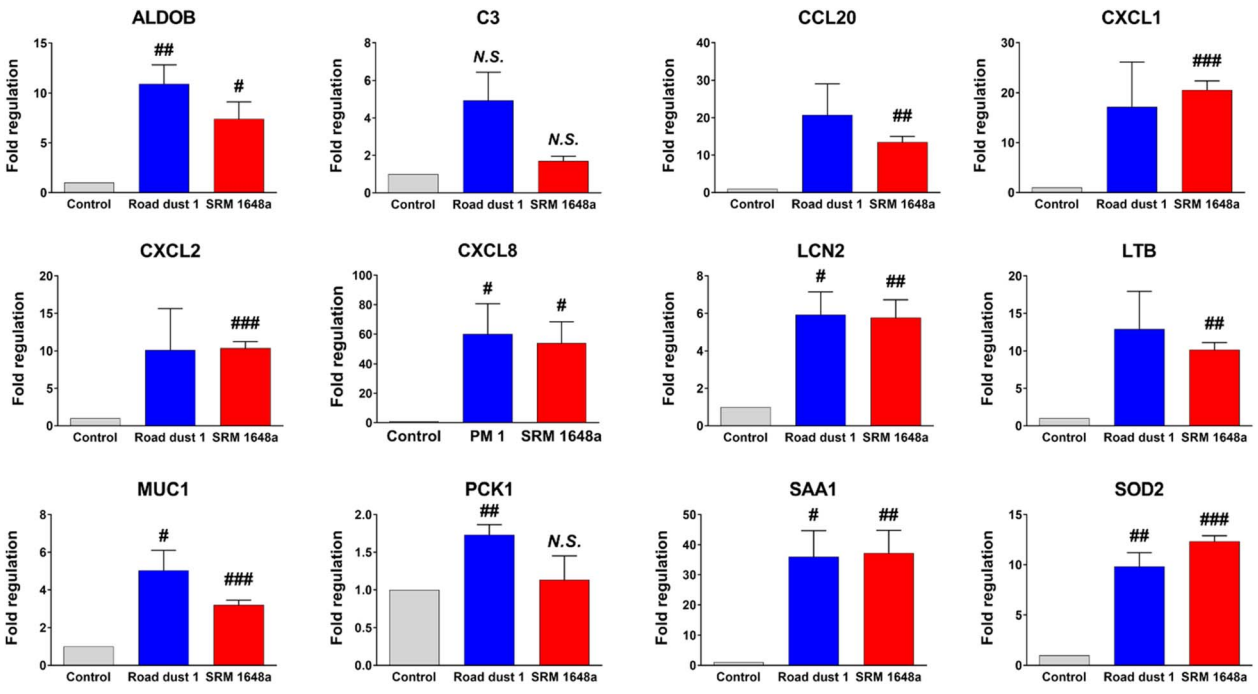

Fig. 5 qPCR validation of inflammatory response-related genes from human colon organoids upon addition of road dust. Error bars represent the standard deviation from three independent experiments. *P* value is #: $p < 0.05$, ##: $p < 0.01$, ###: $p < 0.001$.

Open Access Article. Published on 18 yanvar 2023. Downloaded on 01.01.2025 04:59:55.
This article is licensed under a Creative Commons Attribution-NonCommercial 3.0 Unported Licence.

(CXCL)1, CXCL2, CXCL3 and CXCL8 are strong neutrophil chemoattractants and are associated with immune responses.[41,42] Lipocalin-2 (LCN2) is expressed in neutrophils, and binding to NGAL is important in immune responses[43] Lymphotoxin beta (LTB) is an inducer of the inflammatory response[44,45], and an increased level of serum amyloid A1 (SAA1) is associated with inflammatory amyloidosis.[46,47] Increased levels of these genes are all related to an increase in the immune response. As seen in animal studies, road dust also induces an increase in inflammatory responses. In addition, the data suggest that exposure to a very high concentration of road dust may not induce instant significant cytotoxicity in human organs; however, this is not an indication that exposure to a road dust is not serious, as chronic exposure to a road dust can deteriorate human health and induce my inflammatory response in human organs.

Conclusions

In summary, our data suggest that a smaller size with high concentrations of C, S and Pb induced higher cytotoxicity in human colon fibroblast and human colon organoids. In addition, road dust-induced inflammatory responses occurred in human colon organoids, as we observed after chronic exposure *in vivo*. The uniformity of organoids needs to be experimentally improved to serve as a material toxicity evaluation system. In addition, in-depth studies on human organoids are needed to more closely mimic actual human organs; however, our research shows that human colon organoids provide a promising tool for assessing human toxicity induced by various materials, including road dust, as an alternative *in vivo* toxicity evaluation.

Experimental section

Preparation of road dust

The urban particulate matter NIST reference sample (SRM 1648a) was purchased from Sigma-Aldrich (St. Louis, MO, USA). Road dust 1–4 were collected from various sites located in the Republic of Korea as described in previous work.[25] The road dust samples from each site were collected using a vacuum cleaner (GAS 14.4 V-Li, Robert Bosch, Gerlingen, Germany). The collected road dust were homogenized in a polyethylene bag. Within 24 h of sampling, collected road dust samples were filtered through a 100 μm screen and dried for 24 h in a desiccator at ambient temperature. The dried road dust samples were stored at 2 °C before further treatment.

Characterization of road dust

C and S elemental analysis of road dust was described in previous work by Koh and Kim.[26] Briefly, elemental analysis of sieved (<100 μm) road dust samples was conducted with Flash 2000 analyzers (Thermo Fisher Scientific, Waltham, MA, USA). Each sample was analyzed three times, and the relative standard deviation of each triplicate's carbon concentration measurement ranged between 1.4 and 16.7%. Pb composition (wt%) of the road dust was determined with a wavelength dispersive X-ray fluorescence (WD-XRF) analyzer (ZSX Primus II, Rigaku, Tokyo, Japan) in triplicate. Scanned electron microscope (SEM) images of road dust were obtained by FE-SEM (Tescan, Brno, Czech Republic) with an MIRA 3 LMH Inbeam detector (Tescan). The size and zeta potential of MPs were obtained with a particle size analyzer (Litesizer 500, Anton Paar, Graz, Austria).

Road dust toxicity evaluation in 2D and 3D normal colon cell cultures

CCD-18Co normal colon fibroblasts (American Type Culture Collection, Manassas, VA, USA) were grown in DMEM supplemented with 10%/1% penicillin/streptomycin and 0.1% gentamicin (Thermo Fisher Scientific) and cultured at 37 °C with 5% CO_2. CCD-18Co cells with a passage number > 5 were used for experimental consistency. Before being seeded onto a 96-well cell culture plate for cytotoxicity experiments, the cells were washed with DPBS twice and trypsinized with 0.25% trypsin–EDTA (Thermo Fisher Scientific) for 3 minutes. For 2D toxicity evaluation, CCD-18Co cells were seeded in 96-well plates at a density of 5×10^3 cells per well. After 12 h of incubation, various concentrations (0.03, 0.06, 0.12, 0.25, 0, 5, 1 and 2 mg mL^{-1}) of road dust dispersed in water were applied to the cells. After 72 h of exposure, the cells were washed and incubated with DMEM mixed with 10% CCK-8 (Dojindo, Kumamoto, Japan) at 37 °C for 1 h. Absorbance at 450 nm was measured using a SpectraMax M5e multimode microplate reader (Molecular Devices, San Jose, CA, USA). The cytotoxicity of road dust samples was assessed from the relative decrease in absorbance compared to that of the non-road dust-treated control cells. For the 3D toxicity test, 5×10^3 CCD-18Co cells per well were seeded on a 96-well ultralow attachment plate (Corning, Corning, NY, USA) and centrifuged at 200 × *g* for 5 minutes. After 12 h of incubation, water-dispersed road dust were added to each well and further incubated for 72 h. The viability of 3D CCD-18Co was estimated using a 3D cell viability assay kit (3D CellTiter-Glo, Promega, Madison, WI, USA).

Road dust toxicity test with normal colon organoids

Human colon organoids were mixed in an ice-cold mixture of 60% Matrigel matrix (Corning) and 40% intestinal organoid culture media (Stemcell Technologies, Vancouver, Canada). Organoid crypts were placed in a 96-well plate (Corning) and incubated at 37 °C for 10 min. Then, 100 μL of intestinal organoid culture media was added, and the medium was replaced every other day. Organoids were passaged every 7–10 d with a gentle cell dissociation reagent (Stemcell Technologies). Human colon organoids on 96-well cell culture plates were treated with the designated concentrations of road dust. The viability of colon organoids was estimated using a 3D cell viability assay kit. Luminescence was measured with a multimode microplate reader (SpectraMax iD5, Molecular Devices, San Jose, CA, USA). To measure the cell death of human colon organoids induced by road dust, we used a live/dead (L/D) cell viability assay kit (Thermo Fisher Scientific, Waltham, MA, USA)

© 2023 The Author(s). Published by the Royal Society of Chemistry

Open Access Article. Published on 18 yanvar 2023. Downloaded on 01.01.2025 04:59:55.
This article is licensed under a Creative Commons Attribution-NonCommercial 3.0 Unported Licence.

and subsequent fluorescence microscopy (Lionheart FX, Winooski, USA). For live/dead fluorescence images, colon organoids were stained in medium containing 5 μM ethidium homodimer (EthD-1) and 5 μM calcein-acetoxymethyl ester (calcein-AM). After 30 min of incubation at 37 °C, road dust were washed 4 times, and the organoids were analyzed under a Lionheart FX fluorescence microscope.

Road dust oxidative stress test with normal colon organoids

ROS generation from colon organoids was measured using cell permeable CellROX Deep Red dye (Life Technologies Corp., Grand Island, NY, USA). For the evaluation of oxidative stress on road dust, approximately 50 colon organoids were seeded per Matrigel dome. Organoids were expanded for 8–9 days in an incubator (37 °C, 5% CO_2) before performing treatments. Media containing 5 μM CellROX Deep Red dye was added to each well, and the cells were incubated at 37 °C and 5% CO_2 for 60 min. Media containing CellROX stain was removed, and the wells were washed with media and fixed with 4% paraformaldehyde for 10 min at RT.

qPCR analysis of road dust-treated human colon organoids

Total RNA isolation of colon organoids was conducted with an RNeasy Mini Kit (Qiagen, Hilden, Germany) following the manufacturer's protocols. RNA quantity and quality were evaluated with a NanoDrop 2000 spectrophotometer (Thermo Fisher Scientific). Two micrograms of RNA from colon organoids was reverse transcribed to cDNA using the RT2 First Strand Kit (Qiagen). The expression of 84 key colon inflammation-related genes was evaluated using Human CD RT2 Profiler PCR Arrays (#PAHS-169Z; Qiagen) and with RT2 SYBR Green ROX qPCR Mastermix (Qiagen) using a Rotor gene Q real-time cycler (Qiagen). The expression level of each gene was normalized to the geometric mean of five housekeeping reference genes (HPRT1, ACTB, RPLP0, B2 M and GAPDH) based on RefFinder (GeneGlobe, Qiagen). A list of qPCR forward and reverse primers used for ALDOB, C3, CCL20, CXCL2, CXCL8, LCN2, LTB, MUC1, PCK1, SAA1 and SOD2 is described in Table S3† (Bioneer, Daejeon, Republic of Korea).

Bright-field microscopy

Images of 2D/3D normal colon cells and colon organoids were obtained using an Eclipse Ti2 inverted microscope (Nikon, Tokyo, Japan) and Lionheart FX automated microscope (Biotek, Winooski, VT, USA).

Statistical analysis

Statistical analysis was performed using GraphPad Prism 9 (GraphPad Software, San Diego, CA, USA) and Origin 8.5 (OriginLab Corporation, Northampton, MA, USA). Each experiment was performed in triplicate unless indicated and values are expressed as the mean ± standard deviation (SD). Statistical significance is denoted as # for $p < 0.05$, ## for $p < 0.01$ and ### for $p < 0.001$.

Conflicts of interest

The authors declare no competing financial interest.

Acknowledgements

The authors greatly acknowledge financial support from the Technology Innovation Program at the Ministry of Trade, Industry and Energy (20009774), Ministry of Science and ICT (2021R1A2C201119512) and the Korea Research Institute of Chemical Technology (SI2231-40) of the Republic of Korea.

References

1 A. Mukherjee and M. Agrawal, *Environ. Chem. Lett.*, 2017, **15**, 283–309.
2 J. D. Sacks, L. W. Stanek, T. J. Luben, D. O. Johns, B. J. Buckley, J. S. Brown and M. Ross, *Environ. Health Perspect.*, 2011, **119**, 446–454.
3 F. Dominici, Y. Wang, A. W. Correia, M. Ezzati, C. A. Pope and D. W. Dockery, *Epidemiology*, 2015, **26**, 556–564.
4 G. Zhang, C. Ding, X. Jiang, G. Pan, X. Wei and Y. Sun, *Sci. Rep.*, 2020, **10**, 7654.
5 M. Steenhof, I. Gosens, M. Strak, K. J. Godri, G. Hoek, F. R. Cassee, I. S. Mudway, F. J. Kelly, R. M. Harrison, E. Lebret, B. Brunekreef, N. A. Janssen and R. H. Pieters, *Part. Fibre Toxicol.*, 2011, **8**, 26.
6 J. E. Mirowsky, L. Jin, G. Thurston, D. Lighthall, T. Tyner, L. Horton, K. Galdanes, S. Chillrud, J. Ross, K. E. Pinkerton, L. C. Chen, M. Lippmann and T. Gordon, *Atmos. Environ.*, 2015, **103**, 256–262.
7 I. M. Dijkhoff, B. Drasler, B. B. Karakocak, A. Petri-Fink, G. Valacchi, M. Eeman and B. Rothen-Rutishauser, *Part. Fibre Toxicol.*, 2020, **17**, 35.
8 S. Y. Kyung and S. H. Jeong, *Tuberc. Respir. Dis.*, 2020, **83**, 116–121.
9 S. Balasubramanian, N. G. G. Domingo, N. D. Hunt, M. Gittlin, K. K. Colgan, J. D. Marshall, A. L. Robinson, I. M. L. Azevedo, S. K. Thakrar, M. A. Clark, C. W. Tessum, P. J. Adams, S. N. Pandis and J. D. Hill, *Environ. Res. Lett.*, 2021, **16**, 103004.
10 L. Kish, N. Hotte, G. G. Kaplan, R. Vincent, R. Tso, M. Gänzle, K. P. Rioux, A. Thiesen, H. W. Barkema, E. Wine and K. L. Madsen, *PLoS One*, 2013, **8**, e62220.
11 E. A. Mutlu, P. A. Engen, S. Soberanes, D. Urich, C. B. Forsyth, R. Nigdelioglu, S. E. Chiarella, K. A. Radigan, A. Gonzalez, S. Jakate, A. Keshavarzian, G. S. Budinger and G. M. Mutlu, *Part. Fibre Toxicol.*, 2011, **8**, 19.
12 E. A. Mutlu, I. Y. Comba, T. Cho, P. A. Engen, C. Yazıcı, S. Soberanes, R. B. Hamanaka, R. Niğdelioğlu, A. Y. Meliton, A. J. Ghio, G. R. S. Budinger and G. M. Mutlu, *Environ. Pollut.*, 2018, **240**, 817–830.
13 J. L. Opstelten, R. M. J. Beelen, M. Leenders, G. Hoek, B. Brunekreef, F. D. M. van Schaik, P. D. Siersema, K. T. Eriksen, O. Raaschou-Nielsen, A. Tjønneland, K. Overvad, M.-C. Boutron-Ruault, F. Carbonnel, K. de Hoogh, T. J. Key, R. Luben, S. S. M. Chan, A. R. Hart,

Open Access Article. Published on 18 yanvar 2023. Downloaded on 01.01.2025 04:59:55.
This article is licensed under a Creative Commons Attribution-NonCommercial 3.0 Unported Licence.

H. B. Bueno-de-Mesquita and B. Oldenburg, *Dig. Dis. Sci.*, 2016, **61**, 2963–2971.
14 J. E. Sellner, The Influence of Fine Particulate Matter on Inflammatory Bowel Disease In South Carolina: An Ecological Analysis, Master's thesis, University of South Carolina, 2016, **https://scholarcommons.sc.edu/etd/3793**.
15 L. Kish, N. Hotte, G. G. Kaplan, R. Vincent, R. Tso, M. Gänzle, K. P. Rioux, A. Thiesen, H. W. Barkema, E. Wine and K. L. Madsen, *PLoS One*, 2013, **8**, e62220.
16 T. Sato, D. E. Stange, M. Ferrante, R. G. J. Vries, J. H. van Es, S. van den Brink, W. J. van Houdt, A. Pronk, J. van Gorp, P. D. Siersema and H. Clevers, *Gastroenterology*, 2011, **141**, 1762–1772.
17 E. d'Aldebert, M. Quaranta, M. Sébert, D. Bonnet, S. Kirzin, G. Portier, J.-P. Duffas, S. Chabot, P. Lluel, S. Allart, A. Ferrand, L. Alric, C. Racaud-Sultan, E. Mas, C. Deraison and N. Vergnolle, *Front. Cell Dev. Biol.*, 2020, **8**, 363.
18 J. Kim, B.-K. Koo and J. A. Knoblich, *Nat. Rev. Mol. Cell Biol.*, 2020, **21**, 571–584.
19 *Organoids: a new window into disease, development and discovery*, **https://hsci.harvard.edu/organoids**, accessed, September 8, 2022.
20 T. Matsui and T. Shinozawa, *Front. Genet.*, 2021, **12**, 767621.
21 A. L. Caipa Garcia, V. M. Arlt and D. H. Phillips, *Mutagenesis*, 2022, **37**, 143–154.
22 F. J. Kelly and J. C. Fussell, *Philos. Trans. R. Soc., A*, 2020, **378**, 20190322.
23 A. Valavanidis, K. Fiotakis and T. Vlachogianni, *J. Environ. Sci. Health, Part C: Environ. Carcinog. Ecotoxicol. Rev.*, 2008, **26**, 339–362.
24 B. Salopek, D. Krasic and S. Filipovic, Measurement and application of zeta-potential, *Rud.-Geol.-Naftni Zb.*, 1992, **4**(1), 147.
25 E.-A. Kim and B. Koh, *Sci. Rep.*, 2020, **10**, 14259.
26 B. Koh and E.-A. Kim, *Environ. Pollut.*, 2019, **255**, 113156.
27 A. Rohr and J. McDonald, *Crit. Rev. Toxicol.*, 2016, **46**, 97–137.
28 *Particulate matter – an overview, ScienceDirect Topics*, **https://www.sciencedirect.com/topics/earth-and-planetary-sciences/particulate-matter**, accessed, September 8, 2022.
29 S. D. Brody and S. Zahran, *Int. J. Epidemiol.*, 2007, **36**, 820–823.
30 E. Resongles, V. Dietze, D. C. Green, R. M. Harrison, R. Ochoa-Gonzalez, A. H. Tremper and D. J. Weiss, *Proc. Natl. Acad. Sci. U. S. A.*, 2021, **118**, e2102791118.
31 X. Li, Y. Zhang, M. Tan, J. Liu, L. Bao, G. Zhang, Y. Li and A. Iida, *J. Environ. Sci.*, 2009, **21**, 1118–1124.
32 J. Feng, Y. Gao, Y. Ji and L. Zhu, Quantifying the interactions among metal mixtures in toxicodynamic process with generalized linear model, *J. Hazard. Mater.*, 2018, **345**, 97–106.
33 J. Feng, Y. Gao, Y. Ji and L. Zhu, *J. Hazard. Mater.*, 2018, **345**, 97–106.
34 L. Shang, K. Nienhaus and G. U. Nienhaus, *J. Nanobiotechnol.*, 2014, **12**, 5.
35 K. Fu, X. Wang, X. Yuan, D. Wang, X. Mi, X. Tan and Y. Zhang, *ACS Omega*, 2021, **6**, 3791–3799.
36 E. Fröhlich, *Int. J. Nanomed.*, 2012, **7**, 5577–5591.
37 R. Gupta and B. Rai, *Sci. Rep.*, 2017, **7**, 45292.
38 N. Li, T. Xia and A. E. Nel, *Free Radical Biol. Med.*, 2008, **44**, 1689–1699.
39 R. S. Gangwar, G. H. Bevan, R. Palanivel, L. Das and S. Rajagopalan, *Redox Biol.*, 2020, **34**, 101545.
40 D. Ricklin, E. S. Reis, D. C. Mastellos, P. Gros and J. D. Lambris, *Immunol. Rev.*, 2016, **274**, 33–58.
41 D. C. T. Palomino and L. C. Marti, *Einstein*, 2015, **13**, 469–473.
42 K. V. Sawant, K. M. Poluri, A. K. Dutta, K. M. Sepuru, A. Troshkina, R. P. Garofalo and K. Rajarathnam, *Sci. Rep.*, 2016, **6**, 33123.
43 T. H. Flo, K. D. Smith, S. Sato, D. J. Rodriguez, M. A. Holmes, R. K. Strong, S. Akira and A. Aderem, *Nature*, 2004, **432**, 917–921.
44 T. Hehlgans, B. Stoelcker, P. Stopfer, P. Müller, G. Cernaianu, M. Guba, M. Steinbauer, S. A. Nedospasov, K. Pfeffer and D. N. Männel, *Cancer Res.*, 2002, **62**, 4034–4040.
45 Y. Shou, E. Koroleva, C. M. Spencer, S. A. Shein, A. A. Korchagina, K. A. Yusoof, R. Parthasarathy, E. A. Leadbetter, A. N. Akopian, A. R. Muñoz and A. V. Tumanov, *Front. Immunol.*, 2021, **12**, 712632.
46 G. H. Sack, *Mol. Med.*, 2018, **24**, 46.
47 R. D. Ye and L. Sun, *J. Leukoc. Biol.*, 2015, **98**, 923–929.

© 2023 The Author(s). Published by the Royal Society of Chemistry